Research Article

ADVANCED PHOTONICS

Large-scale optical programmable logic array for two-dimensional cellular automaton

Wenkai Zhang,[a,†] Bo Wu,[a,†] Wentao Gu,[a] Junwei Cheng,[a] Hailong Zhou,[a,*] Dongmei Huang,[b,c] Ping-kong Alexander Wai,[d] Liao Chen,[a] Wenchan Dong,[a] Jianji Dong,[a,*] and Xinliang Zhang[a]

[a]Huazhong University of Science and Technology, Wuhan National Laboratory for Optoelectronics, School of Optical and Electronic Information, Wuhan, China

[b]The Hong Kong Polytechnic University Shenzhen Research Institute, Shenzhen, China

[c]The Hong Kong Polytechnic University, Photonics Research Institute, Department of Electrical and Electronic Engineering, Hong Kong, China

[d]Hong Kong Baptist University, Department of Physics, Hong Kong, China

Abstract. Despite more than 40 years of development, it remains difficult for optical logic computing to support more than four operands because the high parallelism of light has not been fully exploited in current methods that are restrained by inefficient optical nonlinearity and redundant input modulation. In this paper, we propose a large-scale optical programmable logic array (PLA) based on parallel spectrum modulation. By fully exploiting the wavelength resource, an eight-input PLA is experimentally demonstrated with 256 wavelength channels. And it is extended to nine-input PLA through the combination of wavelength's and spatial dimensions. Based on PLA, many advanced logic functions like 8-256 decoder, 4-bit comparator, adder and multiplier, and state machines are first realized in optics. We implement the two-dimensional optical cellular automaton (CA) for what we believe is the first time and run Conway's Game of Life to simulate the complex evolutionary processes (pulsar explosion, glider gun, and breeder). Other CA models, such as the replicator-like evolution and the nonisotropic evolution to generate the Sierpinski triangle are also demonstrated. Our work significantly alleviates the challenge of scalability in optical logic devices and provides a universal optical computing platform for two-dimensional CA.

Keywords: optical computing; programmable logic array; optical cellular automaton.

Received Apr. 8, 2024; revised manuscript received Aug. 11, 2024; accepted for publication Sep. 10, 2024; published online Oct. 17, 2024.

[DOI: 10.1117/1.AP.6.5.056007]

1 Introduction

Today, the demand for computing is rapidly increasing, but the development of electronic computing faces major challenges of power consumption and latency that cannot meet the requirements of high-density computing. Compared to electronic computing, optical computing offers the potential advantages of high speed, low power consumption, and high parallelism.[1–3] Since Boolean logic is the cornerstone of modern digital computing systems, many attempts have been made to implement logic operations optically for more than 40 years.[4–10] However, most optical logic schemes can only support no more than four input operands because the nonlinear requirement in optical logic severely impedes the optimal utilization of optical parallelism. The limited bit width confines optical logic applications to some basic logic functions, such as the two-input logic gates,[11,12] 2-4 decoder,[13–15] one- or two-bit adder,[16–18] comparator,[19–21] and multiplier.[22] Many advanced logic functions, such as large-scale state machines and two-dimensional (2D) cellular automaton (CA), are still difficult to implement on the optical platform.

Considering the binary states (live or dead) of cells in most CAs can be represented by the logic levels (Logic 1 or 0), CA is a suitable model executed by logic devices, which can emulate various complex dynamical behaviors by interacting with surrounding cells.[23,24] It has been widely applied in numerous fields

*Address all correspondence to Hailong Zhou, hailongzhou@hust.edu.cn; Jianji Dong, jjdong@hust.edu.cn

†These authors contributed equally to this work.

such as the simulation of traffic flow,[25,26] forest fires,[27] and physical and chemical phenomena.[28,29] Especially, as one of the most popular CA models, Conway's Game of Life is designed to simulate the evolutionary process of cells[30] and exhibits emergent and self-organized behavior.[31,32] The Turing universality of Conway's Game of Life has also been demonstrated, and thus it can simulate everything algorithmically computable with appropriate initial states.[33–35] With the increase in the number of iterations and involved cells, the evolution of complex models necessitates large amounts of computing resources. To alleviate this issue, the pioneering work attempts to construct photonic CAs with discrete optical components.[36] However, it can only support one-dimensional CAs and requires the relevant electronic device to perform nonlinear computing. The more complex models, including Conway's Game of Life (one of the 2D CAs), cannot be executed on it and the reliance on electronic computing will reduce the benefits brought by light.

In virtue of its reconfigurability and universality, the optical programmable logic array (PLA) has the potential to construct the universal optical platform for the simulation of CA. Its digital computing features also obviate the involvement of electronic nonlinear computing. However, the state-of-the-art optical PLA schemes are confined to a small scale regardless of the all-optical (AO) or electronic-optical (EO) methods. The AO methods utilize nonlinear effects like four-wave mixing in highly nonlinear optical fibers[37,38] or semiconductor optical amplifiers[39] to perform logic AND operations between input signals and generate the logic minterms. The limited parallelism and low efficiency of AO nonlinear effects restrain the scalability of AO PLA. The AO PLA can only support three input operands with a maximum of eight wavelengths.[40] The EO methods tend to generate logic minterms by controlling the on/off states of serial microring resonators based on the EO nonlinear effect, which can be seen as optical logic AND operations between the input electronic signals.[41] Despite avoiding optical nonlinearity, the output Logic 1 has multiple levels and the number of required microring modulators is proportional to the square of the number of input operands. Limited by the massive redundant input modulators, the number of input operands and the corresponding wavelengths demonstrated to date has not exceeded four.[42,43] As a result, Conway's Game of Life cannot be executed in the current optical PLA. The limited input operands hinder the further development and practical application of optical PLA not only in optical CA but also in optical digital computing.

In this paper, we experimentally demonstrate a large-scale optical PLA by parallel spectrum modulation and utilize it as a universal optical computing platform for 2D CA. An eight-input PLA is implemented by cascading eight spectral modulators (SMs) with specific square-wave transmission spectra. The generated 256 wavelength channels correspond to 256 logic minterms of eight input operands, which can be selected by wave shapers (WSs) to perform the desired logic outputs. Various advanced logic functions, such as 8-256 decoder, 4-bit comparator, adder, and multiplier are first realized by optical components. And we combine the dimensions of wavelength and space to achieve a nine-input PLA, which is characterized through date state machines. The nine-input PLA is then used to realize the optical 2D CA for the first time and run Conway's Game of Life to simulate the evolutionary process of cells, including pulsar, glider gun, and breeder. Besides, other CA models such as the replicator-like evolution and the nonisotropic evolution to generate the Sierpinski triangle are also demonstrated. Our work paves the way for large-scale optical digital computing and opens a new avenue for the general optical CA computing platform.

2 Results

2.1 Principle of PLA

Generally, any logic function with N-input operands can be constructed by the combination of logic minterms, which is defined as the AND operation of all N operands where any of the operand may be represented by either the operand itself or its complement (NOT). For example, the logic operation A XOR B is composed of two minterms, $A\overline{B}$ and $\overline{A}B$. In each case, only one minterm is Logic 1. The mutually exclusive characteristic of logic minterms ensures the combined logic results will not generate multiple levels. Therefore, a PLA can be implemented by selecting the required minterms and summing them.

Figure 1(a) shows a three-input (signals A, B, C) PLA consisting of three cascaded SMs. To realize an SM, a wavelength-selective switch (WSS) is first used to partition the incoming spectra into positive (+) and negative (−) channels. Then, a 2×1 optical switch (OS) is used to select the positive or negative channel according to the input logic signal. This allows the SM to produce two complementary square-wave spectra in the states of Logic 0 and Logic 1, respectively. Since three input operands correspond to eight logic minterms, the PLA requires eight different wavelengths from the light source. After SM_1, signal A is loaded on light at wavelengths $\lambda_0 - \lambda_3$ and signal $\overline{A}$ is loaded on light at wavelengths $\lambda_4 - \lambda_7$. The period of the subsequent transmission spectrum of the SM is halved compared to the previous SM, ensuring that all possible combinations of input signals can be mapped to different wavelengths. Thus, the output wavelengths of SM_2 include four logic minterms of signal A and signal B: AB (λ_0, λ_1), $A\overline{B}$ (λ_2, λ_3), $\overline{A}B$ (λ_4, λ_5), $\overline{A}\,\overline{B}$ (λ_6, λ_7). After SM_3, eight logic minterms of the three input operands (A, B, C) are carried on the light at eight different wavelengths. After all logic minterms are generated, the WSs are placed to configure the wavelength channels and output the desired logic functions. The modulation process can also be expressed by the correspondence matrices between the states of input signals and wavelengths shown in Fig. 1(b). The initial input matrix I_{in} is an all-one matrix whose rank equals 1. Having been modulated by three SMs, the output matrix S_3 is a diagonal matrix composed of eight linearly independent wavelength basis vectors. Considering that the three-input logic will have eight output states, the final logic results can be seen as an eight-dimensional vector that can be linearly synthesized by the generated wavelength basis vectors through the following WS.[44] As for N-input PLA, the 2^N logic minterms can be generated with 2^N wavelength channels, and only N modulators are required.

2.2 Demonstration of PLA Functions

Since the WSSs in the experiment allow for wavelength tuning within ~40 nm around the C-band, we choose 256 wavelength channels with 0.15 nm spacing to achieve an eight-input PLA composed of eight cascaded SMs for minterm generation and one WS for minterm combination. The details of the experimental setup are shown in the Supplementary Material 1. Figure 2(a) shows the schematic diagram of the proposed PLA. The minterm generation part consists of eight cascaded SMs, which

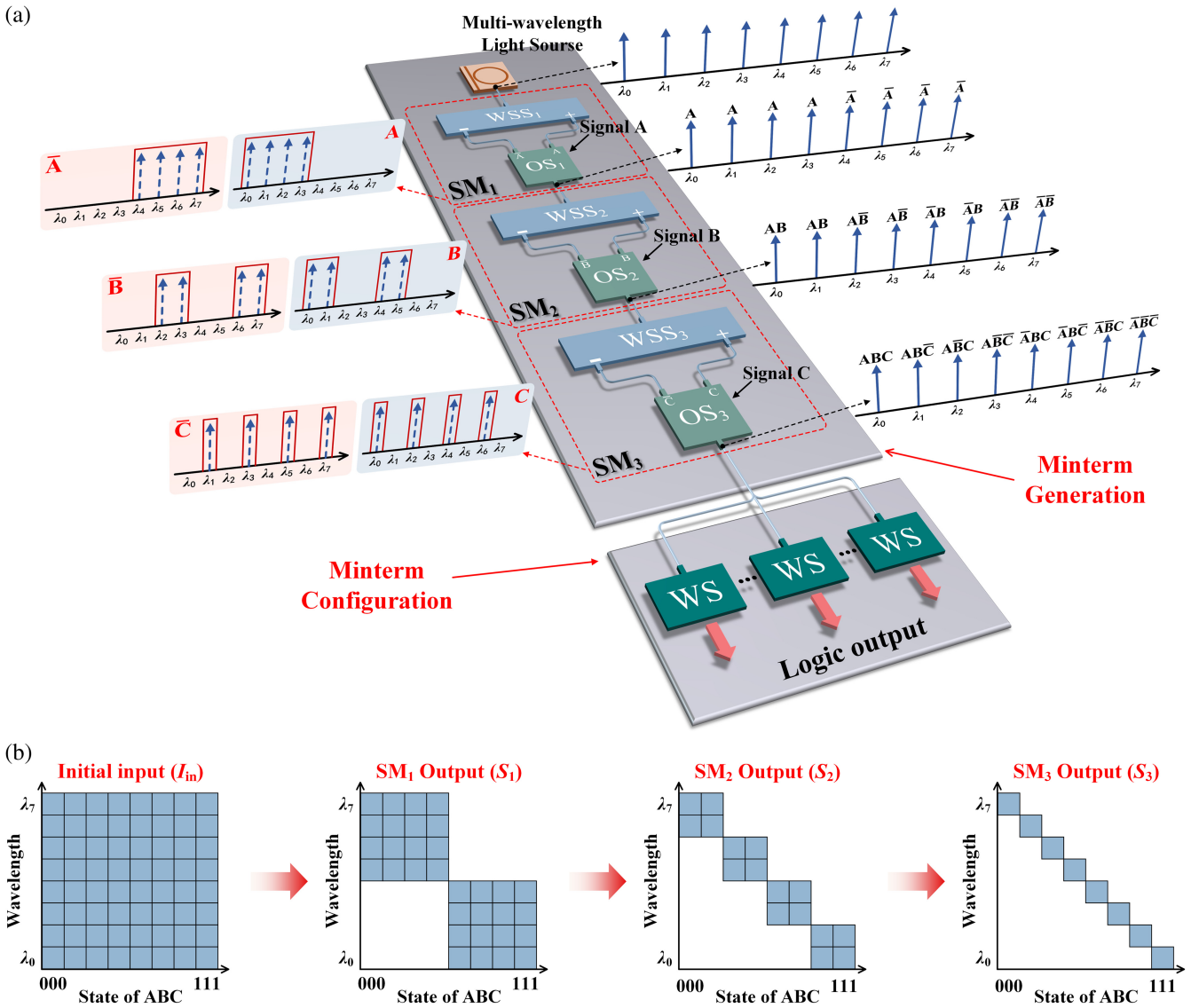

Fig. 1 Operating principle of the proposed PLA based on parallel spectrum modulation. (a) Sketch map of a three-input PLA. (b) The correspondence matrices between the states of input signals and wavelengths. SM, spectral modulator; WSS, wavelength-selective switch; OS, optical switch; WS, wave shaper.

requires 256 eight-input AND gates to generate the complete logic minterms. Here, the method of parallel spectrum modulation fully utilizes the abundant wavelength resources of light, resulting in a significant reduction in the number of devices. The generated minterms are in different wavelength channels, represented by the blue lines in Fig. 2(a). All minterms are generated in one optical path, which also reduces the spatial complexity. As for the configuration part, whether to use the minterms depends on the selection of the corresponding wavelength channels. By summing the selected minterms in the red lines, the PLA will produce the targeted logic results.

We first demonstrate the ability of minterm generation (i.e., 8-256 decoder) of the PLA. The measured confusion matrix in Fig. 2(b) shows that each state of the eight input operands corresponds to one wavelength channel ($I_1, \ldots, I_8$ have 256 states ranging from 0 to 255 in the decimal form). It also shows that each input wavelength channel is independent and represents one logic minterm. The extinction ratio (ER) between each wavelength channel exceeds 17 dB. Figure 2(c) shows the spectra of three different minterms with the minterm generation part. Owing to the background noise of the erbium-doped fiber amplifier (EDFA) placed between the fourth SM and fifth SM, some wavelength channels will produce noise spikes. In the short wavelength region, the efficiency of the EDFA is comparatively decreased and the background noise increases, resulting in a relatively lower ER for these wavelength channels. For some logic functions, PLA requires the selection of multiple wavelength channels. The ER of logic levels will decrease to some degree when the noise spikes appear in these selected channels. This can be enhanced by utilizing lower-noise optical amplifiers. And it is possible to avoid the use of EDFA by increasing the input optical power and using lower-loss WSSs, which can further increase the ER of logic levels.

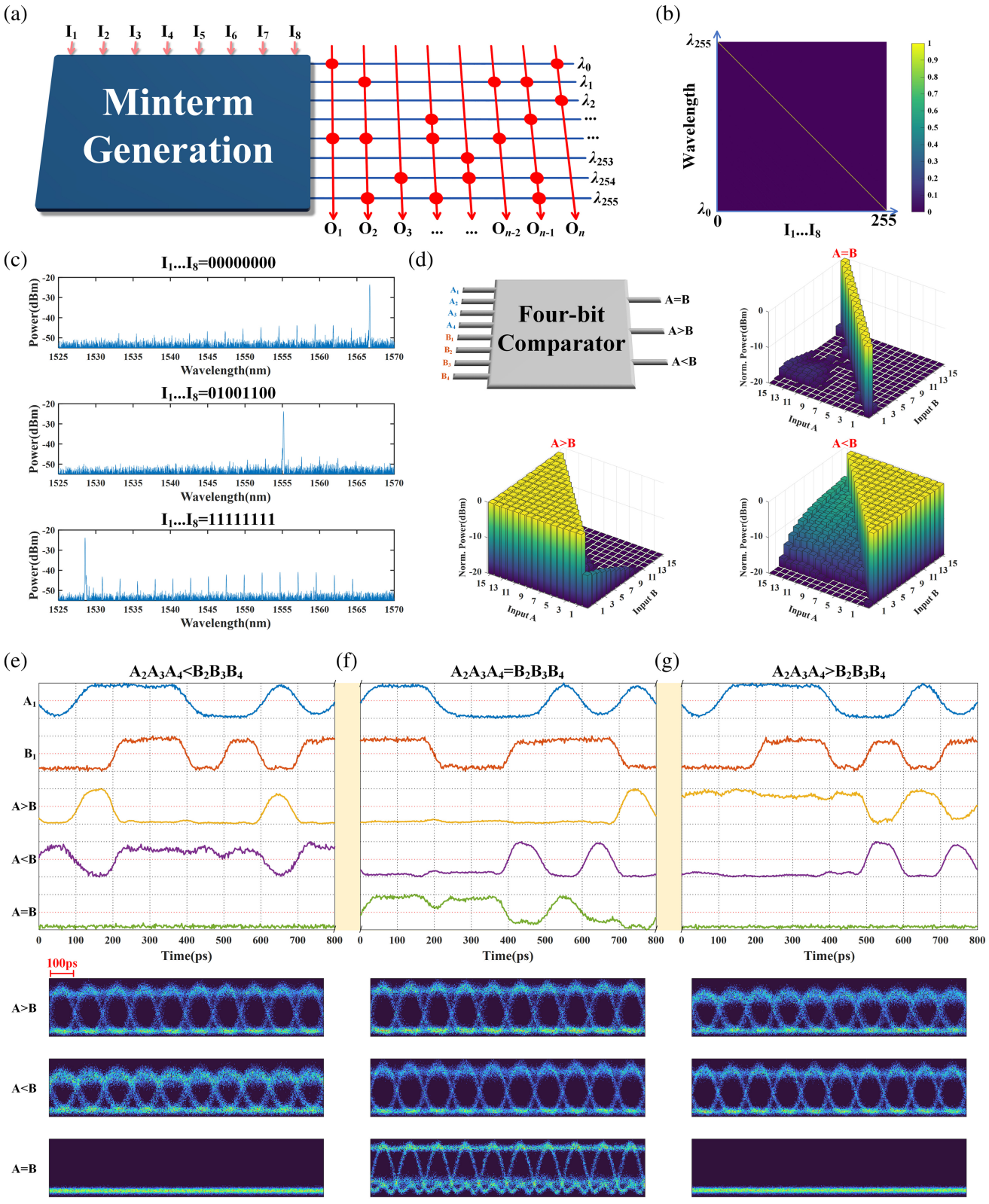

Fig. 2 Performance characterization of the PLA. (a) Schematic diagram for the proposed PLA. (b) Measured confusion matrix between 256 input states and output power of 256 wavelength channels. (c) Output spectra of PLA for three different minterms. (d) Schematic diagram of the 4-bit comparator and the corresponding power distributions of three output ports between input signal A $(A_1A_2A_3A_4)$ and signal B $(B_1B_2B_3B_4)$. Input/output waveforms and output eye diagrams of the comparator in the situations of (e) $A_2A_3A_4 < B_2B_3B_4$, (f) $A_2A_3A_4 = B_2B_3B_4$, and (g) $A_2A_3A_4 > B_2B_3B_4$.

We then configure the PLA to implement a 4-bit comparator, as shown in Fig. 2(d). The input signal A $(A_1A_2A_3A_4)$ and signal B $(B_1B_2B_3B_4)$ can both take a total of 16 integers ranging from 0 to 15 in the decimal form. The power distributions of three output ports in Fig. 2(d) demonstrate the judging logic results between signal A and signal B when traversing all bit states. The logic level's ER is higher than 7 dB, which depends on the quantity and quality of the logic minterms contained in the output channels. After validating the functions of the comparator in all input states, we try to test the comparator with a high-speed data rate. Thus, high-speed optical switches are employed to load bit A_1 and bit B_1 at 10 Gbit/s and other bits of signals A and B are set to fixed values. Figures 2(e)–2(g) show the temporal waveforms of input and output signals and the output eye diagrams of the comparator. The quality of signals will degrade to some extent due to the inconsistent modulation depth of modulators. The accurate execution of the comparison at 10 Gbit/s verifies the high-speed computing ability of the proposed PLA. Other advanced logic functions like 4-bit adder and multiplier are demonstrated in the Supplementary Material 2.

Limited by the resolution and operating wavelength range of the WSSs in the experiment, only 256 wavelength channels are utilized to realize eight-input PLA. We extend to nine-input PLA by adding a 1×2 optical switch in the spatial dimension, shown in Fig. 3(a). The 256 wavelength minterms are first generated by eight cascaded SMs, and then modulated by the 1×2 OS. As a result, the upper port output of OS contains 256 wavelength channels representing minterms with signal I_9, and the lower port outputs 256 minterms with $\overline{I_9}$, which includes all the minterms generated by nine operands. Two WSs follow the OS to select the required minterms. The selected wavelength channels are mixed together by an optical coupler, thereby realizing nine-input logic functions. Based on nine-input PLA, we demonstrate a state machine to deduce the date (month and day) according to the provided day of the year presented in Fig. 3(b). The day of the year (1 to 365) can be expressed by a 9-bit binary number that serves as the input operands of nine-input PLA. The month (1 to 12) and the day of the month (1 to 31) can be converted into a 4-bit binary number and a 5-bit binary number, respectively. We can obtain the final inference results from the outputs of PLA. As an example, we input the 324th day of the year, and get the results of November (1011), 20 (10100), with the ER exceeding 10 dB. Similarly, a reverse state machine can use the date (month and day) as input and output the day of the year depicted in Fig. 3(c). (Truth tables for the proposed state machines are shown in the Supplementary Material 3.)

2.3 PLA for 2D CA

Based on nine-input PLA, we experimentally construct the general optical CA computing platform and perform Conway's Game of Life, whose optical output can directly represent the state of the cell (live or dead) in the next iteration. In the 2D CA, the state of the center cell in the next iteration is determined by the 3×3 cells shown in Fig. 4(a), and the corresponding rules are listed as follows.

(1) If the center cell is surrounded by three live cells, it becomes live in the next iteration, regardless of its current state.

(2) If there are two live cells around the center cell, it remains in its current state in the next iteration.

(3) If the center cell is surrounded by less than two or more than three live cells, it becomes dead in the next iteration, regardless of its current state.

We assign the states of nine cells to the nine input operands $(I_1 - I_9)$ of PLA. If the cell is live, the corresponding input operand takes Logic 1; otherwise, it takes Logic 0. By this means, the evolutionary rules can be transformed into the logic operations executed by PLA, and the logic output is the state of the

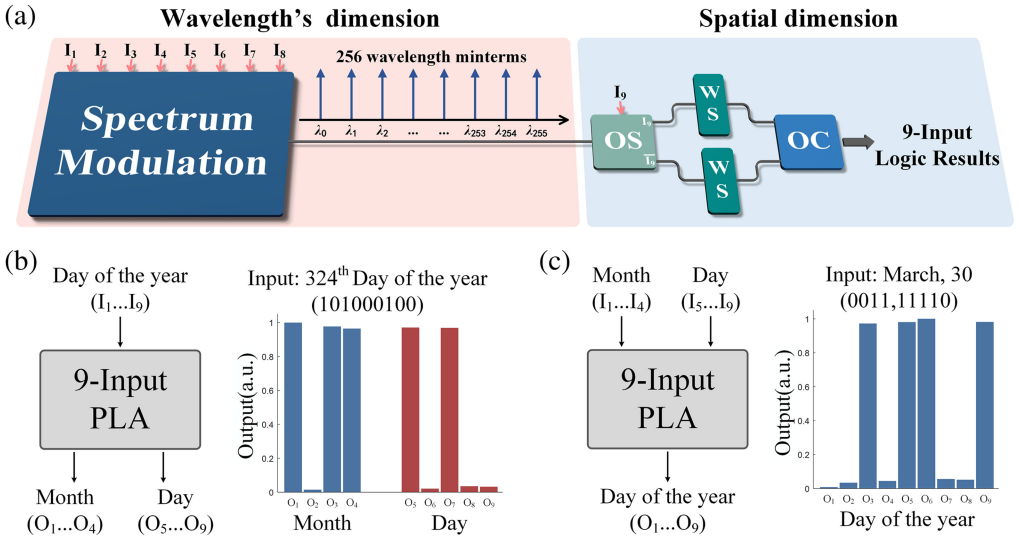

Fig. 3 Demonstration of nine-input PLA. (a) Nine-input PLA realized by combining the wavelength's and spatial dimensions. (b) Statement machine to infer the date (month and day) according to the provided day of the year based on nine-input PLA. The input is 324th (101000100) of the year, and the output is November (1011), 20 (10100). (c) A reverse statement machine to infer the day of the year according to the provided date (month and day). The input is March (0011), 30 (11110), and the output is the 89th (001011001) day of the year. OC, optical coupler.

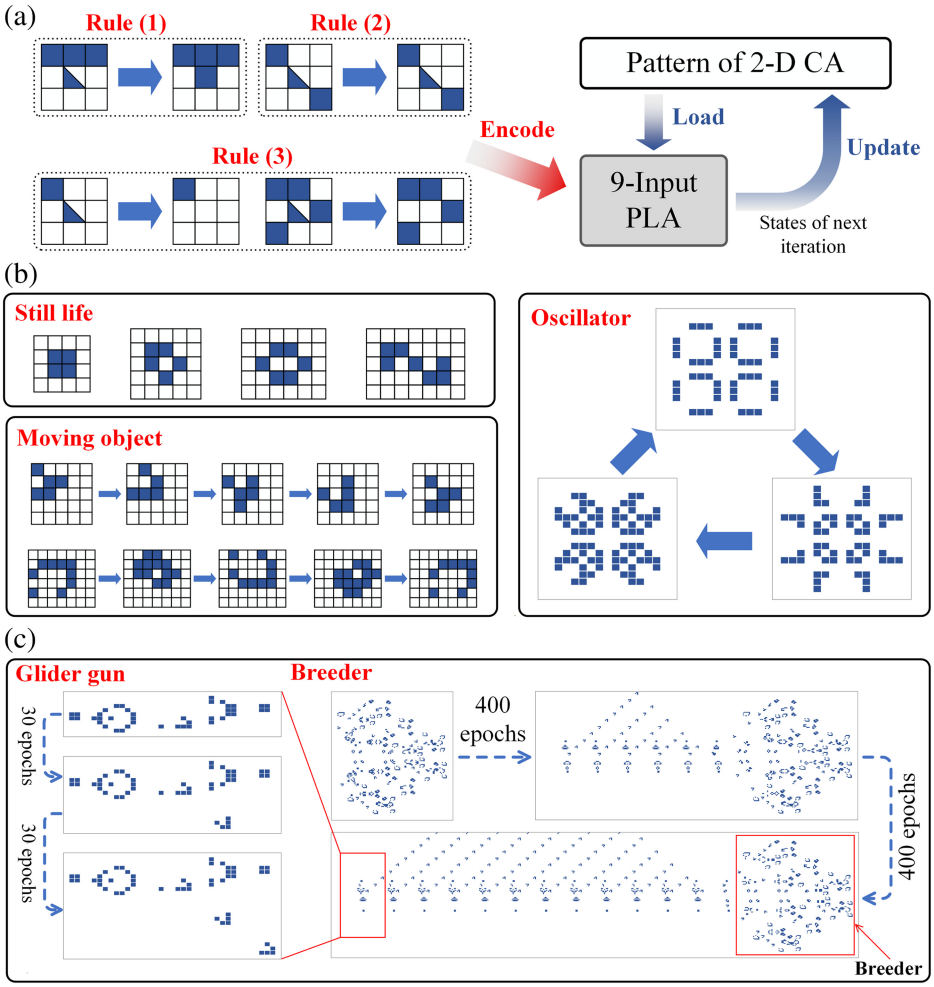

Fig. 4 Operation of Conway's Game of Life on general optical CA computing platform. (a) Schematic for the evolution of Conway's Game of Life executed by nine-input PLA. The evolutionary rules of Conway's Game of Life,[30] in which the two different colors represent the state of the cell (blue represents the live state and white represents the dead state), are programmed into nine-input PLA. The input of PLA is the states of the center cell and surrounding eight cells, and the output is the center cell's state of the next iteration. (b) Three basic models in Conway's Game of Life,[46] including still life (from left to right: block, boat, beehive, and long snake), moving object (glider and light spaceship), and oscillator (pulsar). (c) Complex models of glider gun and breeder implemented by nine-input PLA.

center cell in the next iteration. By shifting the center cell's position, all cells' states will be updated, thus accomplishing one iteration. (Truth tables for the proposed CAs are shown in the Supplementary Material 4.) During the entire evolutionary process, the logic function executed by PLA is fixed. The cells' states are converted to the logic signal and fed into PLA to acquire the next state of the center cell. Figure 4(b) shows three basic models in Conway's Game of Life. The still-life models will consistently retain their shapes throughout the iteration process, which can be seen as stable patterns. There are also moving object models with different moving directions and speed, like the glider that moves diagonally by one cell every four iterations and the light spaceship that moves orthogonally by two cells every four iterations. An oscillator is a pattern that returns to its initial phase after two or more generations. Here, the pattern of pulsar oscillates during three iterations, which looks like the explosion procedure of the pulsar. (See the dynamic evolutionary process of the pulsar in Video 1). We run the complex model of the breeder on the PLA, presented in Fig. 4(c). As the evolution proceeds, the breeder will continually move toward the right and leave glider guns along the way. The generated glider gun will produce gliders every 30 iterations, and the gliders will move diagonally away. (See the dynamic evolution processes of glider gun and breeder in Videos 2 and 3). The above-mentioned models are just the tip of the iceberg in the Game of Life. Our general optical 2D CA computing platform can also realize more complex models like logic circuits[45] and the Turing machine.[34]

Apart from Conway's Game of Life, other kinds of 2D CA are also implemented by the PLA. Figure 5(a) depicts the replicator-like evolution, whose rule can be described as: if the center cell is surrounded by one or three or five or seven live cells, it becomes live in the next iteration, regardless of its current state.

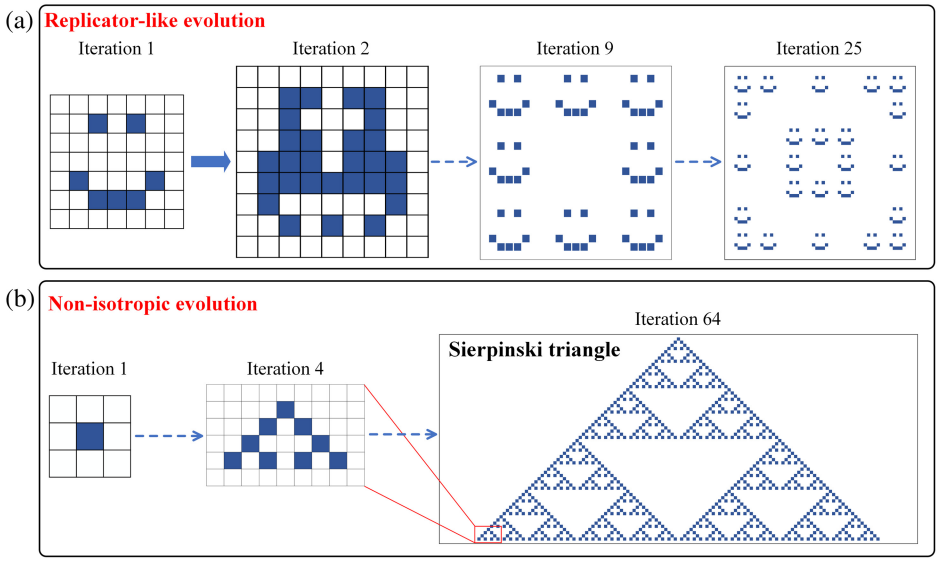

Fig. 5 Other kinds of 2D CAs implemented by the PLA. (a) The replicator-like evolution, in which the smile face copies itself in the iteration process. (b) The nonisotropic evolution, in which a single-cell pattern can create the Sierpinski triangle.

The initial pattern is a smiling face composed of seven live cells. It will replicate itself into eight copies after eight iterations, and more copies will be generated with the progression of iterations. Conway's Game of Life and the replicator-like evolution belong to the isotropic evolution, where the next state of the center cell is equally determined by surrounding cells, regardless of their positions. We demonstrate one of the nonisotropic evolutions, shown in Fig. 5(b). The rules are written as follows.

(1) If the center cell is live, it remains live in the next iteration.
(2) If the center cell is dead, only when the cell on its top-left or top-right is live, can it become live in the next iteration.

Following the rules, a single-cell pattern will create the complex pattern of the Sierpinski triangle, which is a classical fractal.[47] (See the dynamic evolution processes of the replicator-like evolution and the nonisotropic evolution in Videos 4 and 5.) This indicates the proposed optical CA computing platform can simulate complex phenomena. More possible applications of 2D CA like the simulation of pedestrian dynamics,[48] traffic flow,[49] the generation of random numbers,[50] and image processing[51] can be further implemented by nine-input PLA.

3 Discussion

Constrained by the main clock frequency, common electronic logic circuits operate at a maximum frequency of a few gigahertz. The proposed PLA can execute logic functions at 10 GHz and has the potential to achieve an operating frequency of 100 GHz by utilizing thin-film lithium niobate modulators. To generate 2^N logic minterms, the electronic logic circuits require N logic NOT gates and 2^N N-input logic AND gates.[52] As for the proposed PLA, only N active optical switches are required. The transmission of light in WSSs is considered as a passive process. Theoretically, the proposed method's power consumption per bit of logic operations can be optimized to 0.163 pJ with the state-of-the-art technology.[53–56] (The detailed estimation of power consumption is provided in the Supplementary Material 5.) In addition, the power consumption has a cubic correlation with the operating frequency in electronic circuits while it has a linear correlation in optical circuits.[10] The proposed PLA has the potential advantages in both computing speed and power consumption compared with its electronic counterparts.

It is highly challenging for the existing methods to realize large-scale optical PLA, including AO and EO methods. For AO PLAs, there is no available optical nonlinearity that allows for the nine-input AND gate to generate logic minterms. Even though the desired nonlinearity exists, the AO PLA still needs 512 nonlinear operations to obtain all the minterms. For EO PLAs, the 81 modulators are required to construct nine-input PLA, and the output waveforms will have multiple levels (an electronic decision is necessary), which greatly impedes practical applications. Table 1 shows the comparison between the proposed nine-input PLA and existing methods, including AO and EO PLAs. The number of modulators is linearly related to the number of input operands in the proposed PLA, making it practical to support more inputs. The remarkable expansion of generated minterms and functions highlights the tremendous progress of optical PLA. Moreover, the number of PLA's inputs

Table 1 Comparison between the proposed PLA and existing methods.

Method	Input operands	Minterms	Functions	Modulators for N operands
AO PLA[40]	3	8	2^8	—
EO PLA[42,43]	4	16	2^{16}	N^2 (multiple high levels)
Proposed PLA	9	512	2^{512}	N

can be increased by increasing the number of wavelength channels, which can be achieved by broadening the wavelength range or narrowing the wavelength channel interval. However, narrowing the wavelength channel interval will decrease the operating speed because a high-speed signal requires a large bandwidth. Thus, there is a trade-off between the operating speed and the number of operands. Here, we estimate the scale of the PLA when the wavelength range is 1500–1635 nm and the wavelength channel interval is 1 GHz. The total bandwidth can be written as

$$\Delta f = \frac{c}{\lambda_1} - \frac{c}{\lambda_2} = 16{,}502.3 \text{ GHz}, \tag{1}$$

where $\lambda_1 = 1500$ nm and $\lambda_2 = 1635$ nm. The maximum number of wavelength channels (W) is ~16,502. The number of input operands N is given as

$$N = [\log_2 W] = 14. \tag{2}$$

Apart from the wavelength's dimension, the introduction of spatial dimensions can further extend the PLA's scale (see more details in the Supplementary Material 6). Provided that the spatial dimension allows for two additional operands, the proposed PLA can support 16 input operands, which is significant for programmable logic devices. Moreover, other dimensions of light, such as polarization and mode, can also be exploited to expand the scale of PLA.

Currently, most CA models are simulated by the corresponding software in traditional electronic computers. When changing the evolutionary rules, it is necessary to recompile. The proposed optical CA platform is directly based on the physical structure, and the transition between different models can be implemented by selecting wavelength channels of PLA, which will reduce the complexity of CA's simulation and configuration. In contrast with the main clock frequency (~GHz) of electronic computers, the higher computing speed (~10 GHz) can further accelerate the CA's evolutionary process. It is inevitable that electronic hardware is still needed for storing the computing results of optical CA, restraining the simulation speed to some extent. Compared with the state-of-the-art optical CA,[36] our scheme not only eliminates the requirement for electronic nonlinear computing, but also achieves a remarkable enhancement in the scale of optical CA. The high ER of PLA allows the output results to directly represent the states of cells. Owing to the implementation of nine-input PLA, we can construct a 2D CA computing platform, which supports 2^{512} (2^{2^9}) possible modes. [The prior optical one-dimensional CA supports 256 (2^{2^3}) possible modes.] The expansion in dimensions also enables the optical CA to simulate more complex evolutionary models like Conway's Game of Life.

Functions supported by the proposed PLA are not limited to those fields mentioned above. Potential applications like encryption and decryption of signals based on XOR operations[57] and optical parity checker[58] can be implemented by PLA. It can also be applied in the optical binary convolutional neural network,[59] where the 3×3 binary convolution kernel can be realized by nine-input PLA.

It is feasible to realize the integration of the proposed PLA. The multi-wavelength source can be the on-chip optical frequency comb, which can produce sufficient wavelength resources and has been widely used in optical computing systems.[60–62] As the key component in PLA, the SM can be fabricated on the chip by using a ring-assisted Mach–Zehnder interferometer (MZI)[54] to generate the periodic square transmission spectrum and by using an MZI structure to implement the high-speed wide bandwidth 1×2 optical switch.[63] To configure the targeted logic functions, we can use the microring array or the Bragg grating to select specific wavelengths. By this means, all involved optical components of PLA can be integrated on the chip.

In conclusion, we demonstrate a large-scale PLA and utilize it for 2D CA. Various advanced logic functions, like 8-256 decoder, 4-bit comparator, adder and multiplier, and state machines are, experimentally demonstrated by configuring the proposed PLA. The high-speed computing capability of 10 Gbit/s has also been verified. Based on nine-input PLA, we construct a general optical CA computing platform and realize the optical 2D CA for the first time. The models (pulsar, glider gun, and breeder) in Conway's Game of Life and other kinds of 2D CA (replicator-like evolution and nonisotropic evolution) are executed by the 2D CA. The proposed PLA greatly expands the current scale of optical logic computing and provides a general CA computing platform for the evolution of complex phenomena.

4 Appendix A: Experimental Setup

The experimental setup is shown in Fig. S1 in the Supplementary Material. The broadband continuous light is first generated by the broadband light source and then shaped by a WS to generate 256 beams in wavelength channels with an interval of 0.15 nm. The SM consists of a WSS and a 1×2 optical switch. By cascading eight SMs, the 256 wavelength channels can load different logic minterms. For the high-speed experiment, the signals are generated by a bit pattern generator, and the results are detected by a 50 GHz photodetector. Owing to the power jitter in a single wavelength channel generated by a broadband light source, the input light in the wavelength channels corresponding to the logic minterms of the targeted logic functions is replaced by the outputs of the lasers.

5 Appendix B: Video Captions

Dynamic evolution processes of 2D CA

Video 1 (mp4; 8.1 kb [URL: https://doi.org/10.1117/1.AP.6.5.056007.s1])
Video 2 (mp4; 46.35 kb [URL: https://doi.org/10.1117/1.AP.6.5.056007.s2])
Video 3 (mp4; 5055.84 kb [URL: https://doi.org/10.1117/1.AP.6.5.056007.s3])
Video 4 (mp4; 46.43 kb [URL: https://doi.org/10.1117/1.AP.6.5.056007.s4])
Video 5 (mp4; 13.64 kb [URL: https://doi.org/10.1117/1.AP.6.5.056007.s5])

Disclosures

The authors declare that they have no conflicts of interest.

Code and Data Availability

The data that support the findings of this study are available from the corresponding authors on reasonable request.

Acknowledgments

This work was supported in part by the National Key Research and Development Program of China (Grant No. 2022YFB2804203), the National Natural Science Foundation of China (Grant Nos. 62075075, 62275088), and the Knowledge Innovation Program of Wuhan-Basic Research (Grant No. 2023010201010049). W.Z., B.W., and H.Z. conceived the idea. W.Z., B.W., and W.G. designed and performed the experiments. H.Z., J.D., J.C., W.Z., and B.W. discussed and analyzed data. W.Z. prepared the manuscript. H.Z., J.D., L.C., W.D., D.H., and P.W. revised the paper, and X.Z. supervised the project. All authors contributed to the writing of the manuscript.

References

1. H. J. Caulfield and S. Dolev, "Why future supercomputing requires optics," *Nat. Photonics* **4**, 261–263 (2010).
2. J. Touch, A.-H. Badawy, and V. J. Sorger, "Optical computing," *Nanophotonics* **6**, 503–505 (2017).
3. C. Li et al., "The challenges of modern computing and new opportunities for optics," *PhotoniX* **2**, 20 (2021).
4. R. A. Athale and S. H. Lee, "Development of an optical parallel logic device and a half-adder circuit for digital optical processing," *Opt. Eng.* **18**, 513–517 (1979).
5. M. N. Islam, "Ultrafast all-optical logic gates based on soliton trapping in fibers," *Opt. Lett.* **14**, 1257–1259 (1989).
6. N. Patel, K. Hall, and K. Rauschenbach, "40-Gbit/s cascadable all-optical logic with an ultrafast nonlinear interferometer," *Opt. Lett.* **21**, 1466–1468 (1996).
7. Q. Xu and M. Lipson, "All-optical logic based on silicon microring resonators," *Opt. Express* **15**, 924–929 (2007).
8. Y. Fu et al., "All-optical logic gates based on nanoscale plasmonic slot waveguides," *Nano Lett.* **12**, 5784–5790 (2012).
9. C. Qian et al., "Performing optical logic operations by a diffractive neural network," *Light: Sci. Appl.* **9**, 59 (2020).
10. Z. Ying et al., "Electronic-photonic arithmetic logic unit for high-speed computing," *Nat. Commun.* **11**, 2154 (2020).
11. Y. Zhang et al., "Chirality logic gates," *Sci. Adv.* **8**, eabq8246 (2022).
12. T. He et al., "On-chip optoelectronic logic gates operating in the telecom band," *Nat. Photonics* **18** (2023).
13. Q. Chen et al., "1 Gbps directed optical decoder based on two cascaded microring resonators," *Opt. Lett.* **39**, 4255–4258 (2014).
14. T. Daghooghi, M. Soroosh, and K. Ansari-Asl, "A novel proposal for all-optical decoder based on photonic crystals," *Photonic Network. Commun.* **35**, 335–341 (2018).
15. H. Alipour-Banaei et al., "A 2*4 all optical decoder switch based on photonic crystal ring resonators," *J. Mod. Opt.* **62**, 430–434 (2015).
16. Z. Ying et al., "Silicon microdisk-based full adders for optical computing," *Opt. Lett.* **43**, 983–986 (2018).
17. J. Dong et al., "Single SOA based all-optical adder assisted by optical bandpass filter: theoretical analysis and performance optimization," *Opt. Commun.* **270**, 238–246 (2007).
18. F. Parandin and M. Reza Malmir, "Reconfigurable all optical half adder and optical XOR and AND logic gates based on 2D photonic crystals," *Opt. Quantum Electron.* **52**, 56 (2020).
19. C. Feng et al., "Toward high-speed and energy-efficient computing: a WDM-based scalable on-chip silicon integrated optical comparator," *Laser Photonics Rev.* **15**, 2000275 (2021).
20. H. Jile, "Realization of an all-optical comparator using beam interference inside photonic crystal waveguides," *Appl. Opt.* **59**, 3714–3719 (2020).
21. Y. Tian et al., "Experimental realization of an optical digital comparator using silicon microring resonators," *Nanophotonics* **7**, 669–675 (2018).
22. W. Dong et al., "All-optical 2×2-bit multiplier at 40 Gb/s based on canonical logic units-based programmable logic array (CLUs-PLA)," *J. Lightwave Technol.* **38**, 5586–5594 (2020).
23. S. Wolfram, "Statistical mechanics of cellular automata," *Rev. Mod. Phys.* **55**, 601–644 (1983).
24. S. Wolfram, "Cellular automata as models of complexity," *Nature* **311**, 419–424 (1984).
25. R. Barlovic et al., "Metastable states in cellular automata for traffic flow," *Eur. Phys. J. B-Condens. Matter Comp. Syst.* **5**, 793–800 (1998).
26. D. E. Wolf, "Cellular automata for traffic simulations," *Phys. A: Stat.. Mech. Appl.* **263**, 438–451 (1999).
27. I. Karafyllidis and A. Thanailakis, "A model for predicting forest fire spreading using cellular automata," *Ecol. Model.* **99**, 87–97 (1997).
28. B. Chopard and M. Droz, "Cellular automata model for the diffusion equation," *J. Stat. Phys.* **64**, 859–892 (1991).
29. L. Kier, C. Cheng, and P. Seybold, "Cellular automata models of chemical systems," *SAR QSAR Environ. Res.* **11**, 79–102 (2000).
30. M. Gardner, "Mathematical games: the fantastic combinations of John Conway's new solitaire game "life"," *Sci. Am.* **223**, 120–123 (1970).
31. N. M. Gotts, "Ramifying feedback networks, cross-scale interactions, and emergent quasi individuals in Conway's Game of Life," *Artif. Life* **15**, 351–375 (2009).
32. P. Bak, K. Chen, and M. Creutz, "Self-organized criticality in the Game of Life," *Nature* **342**, 780–782 (1989).
33. P. Rendell, *Collision-Based Computing*, pp. 513–539, Springer (2002).
34. P. Rendell, "A Universal Turing Machine in Conway's Game of Life," in *Int. Conf. High Performance Comput. Simul.*, Istanbul, Turkey, pp. 764–772 (2011).
35. P. Rendell, *Turing Machine Universality of the Game of Life*, Springer (2016).
36. G. H. Li et al., "Photonic elementary cellular automata for simulation of complex phenomena," *Light: Sci. Appl.* **12**, 132 (2023).
37. W. Dong et al., "Canonical logic units using bidirectional four-wave mixing in highly nonlinear fiber," *Photonics Res.* **3**, 164–167 (2015).
38. L. Lei et al., "Expanded all-optical programmable logic array based on multi-input/output canonical logic units," *Opt. Express* **22**, 9959–9970 (2014).
39. W. Dong et al., "Integrated all-optical programmable logic array based on semiconductor optical amplifiers," *Opt. Lett.* **43**, 2150–2153 (2018).
40. W. Dong et al., Simultaneous full set of three-input canonical logic units in a single nonlinear device for an all-optical programmable logic array," *Opt. Express* **30**, 41922–41932 (2022).
41. C. Qiu et al., "Demonstration of reconfigurable electro-optical logic with silicon photonic integrated circuits," *Opt. Lett.* **37**, 3942–3944 (2012).
42. Y. Tian et al., "Reconfigurable electro-optic logic circuits using microring resonator-based optical switch array," *IEEE Photonics J.* **8**, 7801908 (2016).
43. Y. Tian et al., "Experimental demonstration of a reconfigurable electro-optic directed logic circuit using cascaded carrier-injection micro-ring resonators," *Sci. Rep.* **7**, 6410 (2017).
44. W. Zhang et al., "Performing photonic nonlinear computations by linear operations in a high-dimensional space," *Nanophotonics* **12**(15), 3189–3197 (2023).
45. J.-P. Rennard, "Implementation of Logical Functions in the Game of Life," in *Collision-Based Computing*, Springer, pp. 491–512 (2002).
46. N. Johnston and D. Greene, *Conway's Game of Life: Mathematics and Construction*, Nathaniel Johnston (2022).
47. B. B. Mandelbrot and B. B. Mandelbrot, *The Fractal Geometry of Nature*, Vol. **1**, W. H. Freeman, New York (1982).

48. C. Burstedde et al., "Simulation of pedestrian dynamics using a two-dimensional cellular automaton," *Phys. A: Stat. Mech. Appl.* **295**, 507–525 (2001).
49. S. i. Tadaki and M. Kikuchi, "Self-organization in a two-dimensional cellular automaton model of traffic flow," *J. Phys. Soc. Jpn.* **64**, 4504–4508 (1995).
50. M. Tomassini, M. Sipper, and M. Perrenoud, "On the generation of high-quality random numbers by two-dimensional cellular automata," *IEEE Trans. Comput.* **49**, 1146–1151 (2000).
51. D. R. Nayak, P. K. Patra, and A. Mahapatra, "A survey on two dimensional cellular automata and its application in image processing," arXiv:1407.7626 (2014).
52. I. W. Damaj, *Programmable Logic Arrays*, Wiley Encyclopedia of Computer Science and Engineering (2007).
53. P. Yang et al., "High-bandwidth lumped Mach-Zehnder modulators based on thin-film lithium niobate," *Photonics* **11**, 399 (2024).
54. A. Rizzo et al., "Ultra-broadband interleaver for extreme wavelength scaling in silicon photonic links," *IEEE Photonics Technol. Lett.* **33**, 55–58 (2020).
55. M. He et al., "High-performance hybrid silicon and lithium niobate Mach–Zehnder modulators for 100 Gbit s^{-1} and beyond," *Nat. Photonics* **13**, 359–364 (2019).
56. K. Nozaki et al., "Amplifier-free bias-free receiver based on low-capacitance nanophotodetector," *IEEE J. Sel. Top. Quantum Electron.* **24**, 4900111 (2017).
57. X. Zhang et al., "High-speed all-optical encryption and decryption based on two-photon absorption in semiconductor optical amplifiers," *J. Opt. Commun. Networks* **7**, 276–285 (2015).
58. Z. Liu et al., "On-chip optical parity checker using silicon photonic integrated circuits," *Nanophotonics* **7**, 1939–1948 (2018).
59. X. Lin, C. Zhao, and W. Pan, "Towards accurate binary convolutional neural network," in *Proc. 31st Int. Conf. Neural Inf. Process. Sys.*, pp. 344–352 (2017).
60. H. Shu et al., "Microcomb-driven silicon photonic systems," *Nature* **605**, 457–463 (2022).
61. L. Chang, S. Liu, and J. E. Bowers, "Integrated optical frequency comb technologies," *Nat. Photonics* **16**, 95–108 (2022).
62. J. Feldmann et al., "Parallel convolutional processing using an integrated photonic tensor core," *Nature* **589**, 52–58 (2021).
63. P. Dong et al., "Submilliwatt, ultrafast and broadband electro-optic silicon switches," *Opt. Express* **18**, 25225–25231 (2010).

Wenkai Zhang received his BS degree from Huazhong University of Science and Technology (HUST), China, in 2021. He is currently a PhD candidate in Wuhan National Laboratory for Optoelectronics at HUST. His research interests include photonic digital computing, optoelectronic devices and integration, and neuromorphic photonics. His work aims to promote the practical application of photonic computing.

Bo Wu is a PhD student at Huazhong University of Science and Technology, China. Currently, he works on the optimization of optical matrix and monolithic integration of various architectures of photonic computing chips, including optical convolutional neural network, optical recurrent neural network, optical Ising machine, and so on. His work aims to improve the integration density and energy efficiency of optical intelligent computing.

Wentao Gu is a PhD student in optical engineering at Wuhan National Laboratory for Optoelectronics, Huazhong University of Science and Technology, China. He is currently conducting research on optical nonlinear effects and optical computing. His work aims to leverage nonlinear effects to achieve more energy-efficient and faster optical computing.

Junwei Cheng is a PhD student at HUST, China. He received his BEng degree from HUST in 2019. Currently, He specializes in developing optical neural networks based on silicon photonics platform. His work aims to provide efficient computing hardware for artificial intelligence applications.

Hailong Zhou received his undergraduate training in optics engineering from HUST and got a PhD from HUST in 2017, and now works as an associate professor at Wuhan National Laboratory for Optoelectronics in HUST. He is mainly engaged in the research of optical matrix computation and its application, including optical neural computation and optical logic computation. In recent years, he has published more than 30 SCI academic papers.

Dongmei Huang received her PhD from The Hong Kong Polytechnic University, Kowloon, Hong Kong, China, in 2020. She is currently an assistant professor in the Photonics Research Institute, Department of Electrical and Electronic Engineering at The Hong Kong Polytechnic University. Her research interests include wavelength swept lasers and their applications in optical coherence tomography and optical sensing systems, ultrafast fiber lasers, integrated photonics, and nonlinear optics.

Ping-kong Alexander Wai received his PhD from the University of Maryland in 1988. He is now a chair professor at Hong Kong Baptist University, Hong Kong, China. He has authored or coauthored over 500 international publications. His research interests include soliton, fiber lasers, modeling and simulations of optical devices, and long-haul optical fiber communications. He is an optica fellow, IEEE fellow, and a fellow of the Hong Kong Academy of Engineering Sciences.

Liao Chen received his PhD from the HUST, Wuhan, China, in 2018. He is currently with the Wuhan National Laboratory for Optoelectronics and School of Optical and Electronic Information, HUST, as a Lecturer. His current research interests include ultrafast spectrum analysis, nonlinear optics, and terahertz science.

Wenchan Dong received her PhD from the HUST, Wuhan, China, in 2018. She is currently with the School of Optical and Electronic Information, HUST, as a Lecturer. Her current research interests include optical computing and signal processing based on integrated devices.

Jianji Dong is a professor at Huazhong University of Science and Technology, where he received his PhD in 2008. He then worked as a postdoctoral research fellow in the Department of Engineering at the University of Cambridge until 2010. His current research focuses on optical computing. In 2024, he was supported by the National Natural Science Foundation for Distinguished Young Scholars of China. He serves as the executive editor of *Frontier of Optoelectronics* and organizes photonics open courses, including a special issue on optoelectronic computing.

Xinliang Zhang received his PhD in physical electronics from the HUST, Wuhan, China, in 2001. He is currently the president of Xidian University and a professor at the Wuhan National Laboratory for Optoelectronics and School of Optical and Electronic Information of HUST. He is the author or coauthor of more than 400 journal articles. His current research interest is optoelectronic devices and integration. In 2016, he was elected as in OSA fellow.